Title: Distinct representational structure and spatial distribution for visual encoding and recall

Wilma A. Bainbridge[1], Elizabeth H. Hall[1,2], Chris I. Baker[1]

1 – Laboratory of Brain and Cognition, National Institute of Mental Health; Bethesda, MD 20814

2 – Department of Psychology, University of California Davis; Davis, CA 95616

Conflict of interest statement: The authors declare no competing financial interests.

Acknowledgements: This research was supported by the Intramural Research Program of the National Institutes of Health (ZIA-MH-002909), under National Institute of Mental Health Clinical Study Protocol 93-M-1070 (NCT00001360).

Abstract

During memory recall, reinstatement is thought to occur as an echoing of the neural patterns during encoding. However, the precise information represented in these recall traces is relatively unknown, with previous work investigating broad distinctions (e.g. scenes versus objects) or individual images, rarely bridging these levels of information. Further, prior work has primarily used cued recall tasks, where this memory trace may reflect a combination of a cue, its paired stimulus, and their association. Using ultra-high-field (7T) fMRI with an item-based recall task, we conducted an in-depth comparison of encoding and recall along a spectrum of granularity, from broad stimulus class (scenes, objects) to object or scene type (e.g., natural, manmade) to individual categories (e.g. living room, cupcake). In the scanner, human participants viewed a trial-unique item, followed by a distractor task, and then visually recalled the initial item. During encoding, we observed decodable information at all levels of granularity in category-selective visual cortex. Conversely, during recall, only stimulus class was decodable in these cortical regions, with the exception of the medial place area. In hippocampus, information was only decodable during perception and only for stimulus class. A closer look within category-selective cortex revealed a segregation between voxels showing the strongest effects during encoding and during recall. Finally, in a whole-brain analysis, we find the strongest evidence for encoding-recall similarity in regions anterior to category-selective cortex. Collectively, these results suggest recall is not merely a reactivation of encoding patterns, displaying a different granularity of information and spatial distribution from encoding.

Introduction

When we recall an object or scene, our memory contains rich object and spatial information (Bainbridge et al., 2019). During such recollection, our brain is thought to reinstate neural patterns elicited by the initial perception (McClelland et al., 1995; Buckner and Wheeler, 2001; Tompary et al., 2016; Dijkstra et al., 2019). One common view is that the hippocampus indexes populations of neocortical neurons associated with that memory (Teyler and Rudy, 2007; Danker and Anderson, 2010; Jonker et al., 2018; Schultz et al., 2019). Under this view, representations in hippocampus are largely independent of a memory's perceptual content (Davachi, 2006; Liang et al., 2013; Huffman and Stark, 2014), while those in neocortex reflect representations elicited during encoding (Kahn et al., 2004; Staresina et al., 2012; Lee et al., 2012; Ison et al., 2015; Ishai et al., 2000; O'Craven and Kanwisher, 2000; Dijkstra et al., 2017). Additional neocortical regions, particularly in parietal cortex, have also shown involvement specific to memory retrieval tasks (Vilberg and Rugg, 2008; Ranganath and Ritchey, 2012; Silson et al., 2019). However, the extent to which representations during recall reflect all the information available during perception is unclear. Here, using ultra-high-field (7T) fMRI, we conducted an in-depth investigation of the content of encoded and recalled representations of objects and scenes across cortex and hippocampus, assessing the granularity of detail in the representations for individual items.

First, we employed a hierarchically organized stimulus set (Figure 1) with three levels of granularity from broad stimulus classes (scenes/objects) to stimulus types (e.g., natural/manmade scenes) to individual items (e.g., bedrooms/conference rooms). Prior work comparing encoding and recall have primarily investigated memory content at opposite ends of this granularity spectrum. At a broad level, recall of stimulus classes (faces, scenes, objects) have been reported to reactivate high-level visual regions (Polyn et al., 2005; Johnson et al., 2009; Reddy et al., 2010; LaRocque et al., 2013) and produce differentiable responses in hippocampus (Ross et al, 2018). At a finer level, other work has shown reinstatement at the individual image or exemplar level, with specific items decodable throughout the neocortex (Dickerson et al., 2007; Buchsbaum et al., 2012; Lee et al., 2012; Kuhl and Chun, 2014) and hippocampus (Zeineh et al., 2003; Gelbard-Sagiv et al., 2008; Chadwick et al., 2010; Wing et al.,

2015; Mack and Preston, 2016; Tompary et al., 2016; Lee et al., 2019). However, it is unclear what information drives discrimination: visual content, semantic content, or memory strength. For example, while recalled grating orientation is decodable from early visual cortex (V1-V3), reinstatement strength but not content is decodable from the hippocampus (Bosch et al., 2014). Our approach using nested levels of stimulus information reveals what granularity of information is contained in these regions, and whether reinstatement is simply an echo of the same response from encoding to recall.

Second, to isolate the activity specific to recall, we adopted a task focusing on recall of individual items without requiring the learning of cue-stimulus associations, which have commonly been used (e.g., Ganis et al., 2004; Kuhl et al., 2012; Zeidman et al., 2015a; Jonker et al., 2018). Recalled representations in associative tasks are likely to contain information not only about the recalled item, but also the cue and the association itself. Further, there are neocortical differences when performing an associative versus item-based memory task (Staresina and Davachi, 2006). In fact, when a target memory is triggered through different associated cues, the reinstated target representations are dissimilar (Xiao et al., 2017). Here, we employ an item-based recall task in which participants encode trial-unique images, and following a distractor task, recall that specific image. This approach allows us to isolate the recall of individual items, without the learning of associations.

Using this direct recall task and nested stimulus structure, we find striking differences in the representational structure and spatial distribution for visual encoding and recall, suggesting recall patterns are not just a repetition of patterns during encoding.

Materials and Methods

Participants

Thirty-four adults were recruited for the experiment. All participants were healthy, right-handed, and had corrected or normal vision. Twelve participants were unable to complete the experiment due to scanner issues, discomfort in the 7T scanner, or time constraints, and their data were excluded from the study; the final set of participants included twenty-two adults (fifteen female). All participants provided consent following the guidelines of the

National Institutes of Health (NIH) Institutional Review Board (NCT00001360, 93M-0170), and were compensated for their participation.

Stimuli

Stimulus images comprised 192 images, 50% objects and 50% scenes, with nested categorical structure (Figure 1a). The objects were made up of four object types, varying along two factors known to show differential responses in the brain during perception: 1) small / big objects (Konkle et al., 2012), and 2) tool / non-tool objects (Valyear et al., 2007; Mahon et al., 2007; Beauchamp and Martin, 2007). Small versus big object categories were defined based on prior literature (Konkle et al., 2012; Bainbridge et al., 2015). Tools were defined as objects commonly grasped by one's hands using a power grip (e.g., Grèzes et al., 2003), although note that there are multiple ways tools are defined in the field (Lewis, 2006). The other half of the stimulus images were scenes, varying along two factors shown to elicit differential responses in the brain: 1) natural / manmade (Park et al., 2011), and 2) open / closed (Kravitz et al., 2011). Each object or scene type contained three categories, with eight exemplars for each object or scene category (e.g., small, non-tool objects: bowl, cupcake, flowers; closed, manmade scenes: bathroom, conference hall, living room). Note that for clarity, we will refer to the most fine-grained level of categorization (e.g., cupcake, bathroom) as stimulus *category*, the mid-level of categorization (e.g., big/small objects, open/closed scenes) as stimulus *type*, and the distinction of objects versus scenes as stimulus *class*. Images were all square 512 x 512 pixel images presented at 8 degrees visual angle, and objects were presented cropped in isolation on a white background.

a)

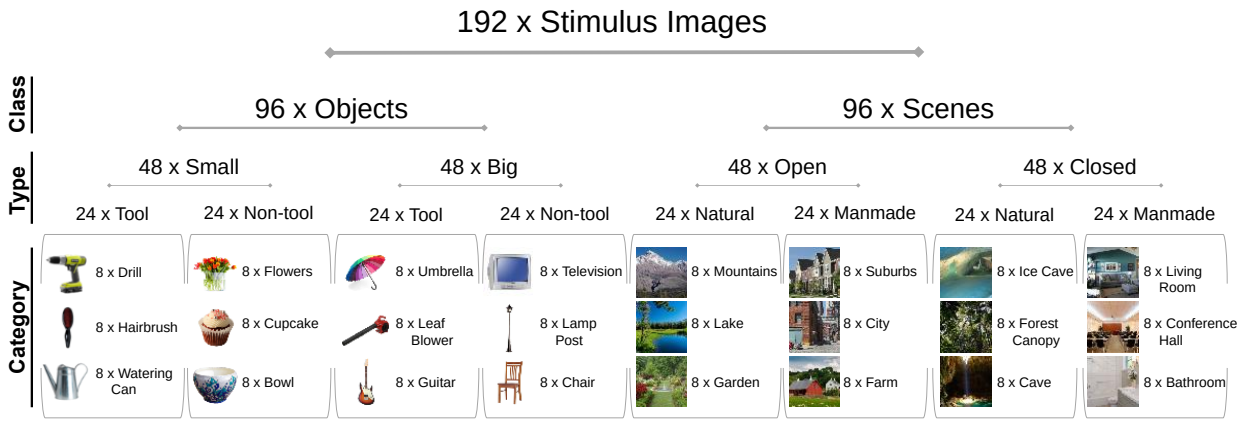

b)

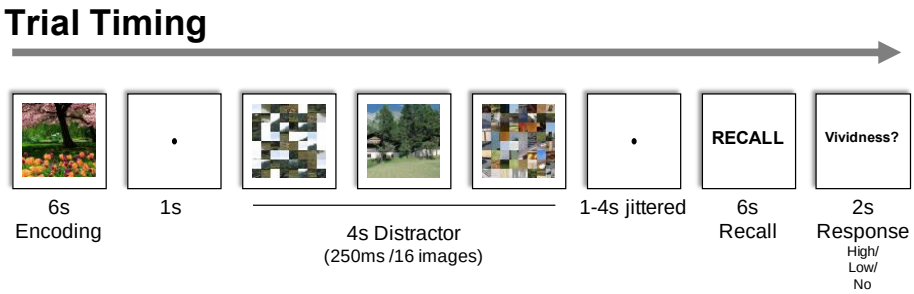

Figure 1. Experimental stimuli and task. (a) Nested structure of stimuli and example images. 192 trial-unique images were encoded and recalled by participants, arranged under nested structure based on broad stimulus *class* (object / scene), stimulus *type* (e.g., open / closed or natural / manmade scene), and stimulus *category* (mountains / lake). Each stimulus category contained 8 different exemplar images (e.g., 8 different lake photographs). (b) The timing of each trial. Participants studied an image for 6 s, performed a distractor task requiring detection of an intact image amongst scrambled images for 4 s, and then after a randomized jitter of 1-4 s, recalled the original image for 6 s. Finally, they indicated the vividness of their memory with a button press.

In-scanner recall task and post-scan recognition task

Participants first participated in a single run of a 7-min 6-sec block-design localizer scan to identify scene- and object-selective regions, using separate stimulus images from the main experiment. They then performed eight runs of an item-based recall memory task (Figure 1b). In each trial, participants studied a stimulus image for 6 s. After a 1 s fixation, they performed a distractor task in which they viewed a stream of 16 quickly presented images (250 ms each), and had to press a button as soon as they saw the sole intact image in a stream of mosaic-

scrambled images. Scrambled and intact target images were taken from a separate stimulus set, and were chosen to be of the same broader stimulus class (i.e., object or scene) as the studied image, but of random type and category. Intact object images were presented as an intact object against a mosaic-scrambled background, so that participants would have to fixate the object to successfully perform the task (rather than identify white edges). The distractor task lasted for 4 s total and was followed by a 1-4 s jittered interval in which participants were instructed to wait and maintain fixation. The word "RECALL" then appeared on the screen for 6 s, and participants were instructed to silently visually recall the originally studied image in as much detail as possible. Finally, following the "RECALL" phase, participants were given 2 s to press a button indicating the vividness of their memory as either no memory, low vividness, or high vividness. The next trial then continued after a 1 s delay. Participants were instructed that the task was difficult, and they should focus on reporting their vividness truthfully and not be concerned about low performance. Each run contained 24 trials, lasting 8 min 38 s, and participants completed 8 runs total. Each run included three "catch trials" that skipped the recall phase, in order to keep participants vigilant and to better separate encoding from distractor and recall phases during deconvolution. Each stimulus category (e.g., guitar, cupcake) was shown once per run, and each stimulus exemplar image was only used once in the entire experiment, so that there would be no memory effects on subsequent presentations of the same image.

After the scan, participants performed a post-scan recognition task to test their memory for the images studied in the scanner. Participants were presented with all 192 images studied in the scanner randomly intermixed with 192 foil images of the same stimulus categories and were asked to indicate for each image whether it was old or new. Two participants were unable to complete the post-scan recognition task due to time constraints.

MRI acquisition and preprocessing

The experiment was conducted at the NIH, using a 7T Siemens MRI scanner and 32-channel head coil. Whole-brain anatomical scans were acquired using the MP2RAGE sequence, with 0.7 mm isotropic voxels. Whole-brain functional scans were acquired with a multiband EPI

scan of in-plane resolution 1.2 x 1.2 mm and 81 slices of 1.2 mm thickness (multiband factor=3, repetition time=2 s, echo time=27 ms, matrix size=160 × 160, field of view=1728 × 1728, flip angle=55 degrees). Slices were aligned parallel with the hippocampus and generally covered the whole brain (when they did not, sensorimotor parietal cortices were not included). Functional scans were preprocessed with slice timing correction and motion correction using AFNI and surface-based analyses were performed using SUMA (Cox, 1996; Saad and Reynolds, 2012). Experimental data were analyzed using generalized linear models (GLMs) across the whole brain, modeling separate regressors for each stimulus category (e.g., cupcake) for the encoding period (6 s boxcar function), distractor period (4 s boxcar), and recall period (6 s boxcar), across even and odd splits of the runs. Each event (e.g., encoding a cupcake) thus had two resulting beta estimates: one across even runs, and one across odd runs. Trials were combined in this way so that the deconvolution for a given recalled item included recall events preceded by different post-distractor jitters, in order to eliminate bleed-over from the encoding or distractor periods. The estimated motion parameters from the motion correction were included as three additional regressors.

FMRI Region of Interest (ROI) Definitions

Key ROIs for early visual cortex, object selective cortex, scene selective cortex, and hippocampus (head/body, tail) were determined *a priori* and defined using functional and anatomical criteria (Figures 3 and 4). Using the independent functional localizer, we identified three scene-selective regions with a univariate contrast of scenes > objects: PPA (Epstein & Kanwisher, 1998), medial place area (MPA; Silson et al., 2016), and occipital place area (OPA; Dilks et al., 2013). We localized object-selective regions lateral occipital (LO) and posterior fusiform (pFs) with a univariate contrast of objects > scrambled images (Grill-Spector et al., 2001). Finally, we localized early visual cortex (EVC) with a univariate contrast of scrambled images > baseline. The ROIs were based on activation within areas defined by the literature (e.g., Epstein and Kanwisher, 1998; Grill-Spector et al., 2001), and were selected first at a threshold of False Discovery Rate (FDR)-corrected threshold of $q = 0.01$, and then selection criteria were gradually relaxed (up to $p=0.05$) until any voxels in that area were found. Left and

right ROIs were combined to create bilateral ROIs. Overlapping voxels between scene- and object-selective regions were discarded. LO, pFs, PPA, and EVC were identified bilaterally in 22 participants, OPA in 21 participants (20 bilateral), and MPA in 20 participants (17 bilateral). Anatomical ROIs were localized using FreeSurfer's recon-all function using the hippocampal-subfields-T1 flag (Iglesias et al., 2015), and then visually inspected for accuracy. Within these anatomical ROIs, we specifically looked at the hippocampus head and body (Hip-HB) versus the tail (Hip-T).

Univariate Analyses

We conducted whole-brain univariate contrasts using GLMs that split the trials into four regressors along two factors: 1) encoding / recall, and 2) scenes / objects. We then performed separate whole-brain T-contrasts of scenes vs. objects during encoding and recall. All whole-brain images were projected onto the cortical surface using AFNI surface mapper SUMA (Saad and Reynolds, 2012).

Representational Similarity Analyses and Discrimination Indices

For multivariate analyses, we investigated the similarity between different types of stimulus information during both encoding and recall, using representational similarity analyses (RSA; Kriegeskorte et al., 2008). For each ROI, we created a representational similarity matrix (RSM) comparing the similarity of all pairs of stimulus category (e.g., cupcake vs. guitar). Similarity was calculated as the Pearson's correlation between the voxel values (t-statistic) in an ROI for one category (e.g., cupcake) from one half of the runs (e.g., odd runs), with the voxel values for another category (e.g., guitar) from the other half (e.g., even runs). Specifically, pairwise item similarity was taken as the average of the correlation with one split (odd runs for item A, even runs for item B) and correlation with the opposite split (even runs for item A, odd runs for item B). This metric indicates the similarity in the neural representations of two categories, and importantly, because the comparisons use separate halves of the data, we can observe a category's similarity to itself across runs. This self-similarity measure thus shows the degree to which a given region shows similarity across exemplars within category (e.g., are

cupcakes similar to other cupcakes). These similarity matrices were created in three ways: 1) correlations of the encoding trials (Encoding RSM), 2) correlations of the recall trials (Recall RSM), 3) correlations of the encoding trials with the recall trials (Cross-Discrimination RSM). These different classifications allow us to see what stimulus information exists separately during encoding and recall, as well as what information is shared between encoding and recall.

From these RSMs, we conducted discriminability analyses, which show the degree to which each ROI can discriminate the different conditions of class, type, and category (e.g., do the responses in PPA discriminate natural vs. manmade scenes?). For each comparison of interest, we computed a discriminability index *D,* calculated as the difference of the mean across-condition correlations (e.g., scenes with objects) from mean within-condition correlations (e.g., scenes with other scenes; Kravitz et al., 2011; Cichy et al., 2014; Harel et al., 2013; Harel et al., 2014; Henriksson et al., 2015). The intuition behind this index is that if an ROI contains information about that comparison, then within-condition similarity should be higher than across-condition similarity (e.g., if the PPA *does* discriminate natural vs. manmade scenes, then natural scenes should be more similar to other natural scenes than manmade scenes). Significant discriminability was determined by a two-tailed t-test comparing discrimination indices across participants versus a null result of 0. Type discriminability was only computed within same-class items (e.g., only scenes were used for the natural vs. manmade comparison), and category discriminability was only computed within same-type items (e.g., when looking at the discriminability of living rooms, they were only compared to other closed, manmade scenes). For the encoding and recall discrimination indices, all statistics reported are FDR-corrected within each ROI at a value of $q < 0.05$ unless noted otherwise. Refer to Figure 2 for a depiction of these discrimination indices and to see example RSMs.

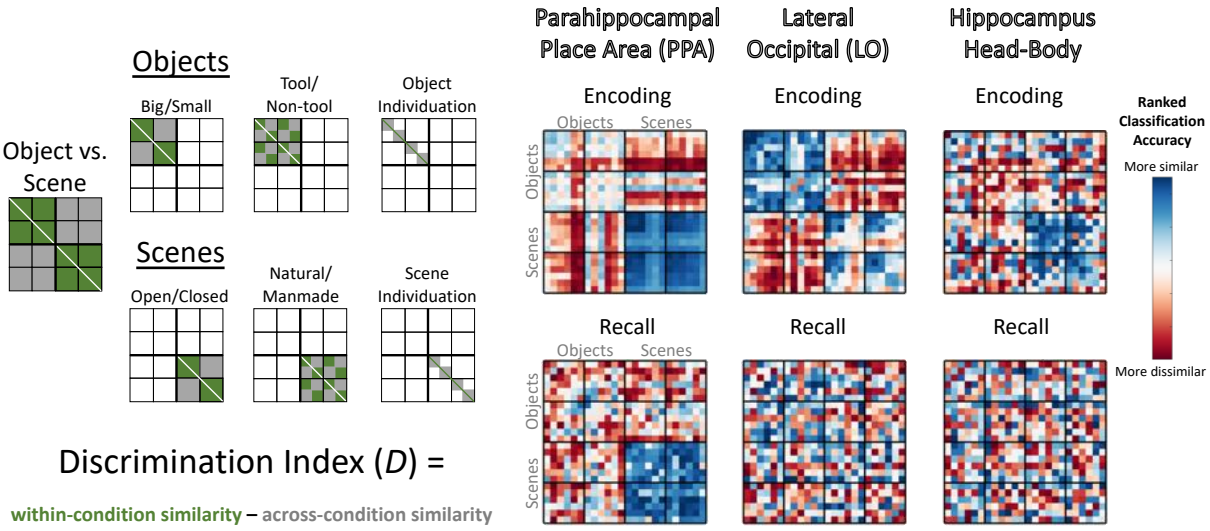

Figure 2 – **Calculating information discriminability from representational similarity matrices.** (Left) Depictions of the cells of the representational dissimilarity matrices (RSMs) used to calculate discrimination indices for key regions of interest (ROIs). The RSMs represent pairwise Pearson's correlations of stimulus groupings calculated from ROI voxel t-values, compared across separate run split halves (odd versus even runs). These depictions show which cells in the matrices are used in the calculation of discriminability of different properties, with green cells indicating within-condition comparisons, which are compared with grey cells indicating across-condition comparisons. For all discriminability calculations except discrimination of individual categories (i.e., individuation), the diagonal was not included. All operations were conducted on the lower triangle of the matrix, although both sides of the diagonal are shown here for clarity. (Right) Examples of encoding and recall RSMs from the data in the current study, specifically the rank-transformed average RSM for the parahippocampal place area (PPA), lateral occipital (LO), and the hippocampus head and body. Blue cells are more similar, while red cells are more dissimilar.

ROI-to-ROI similarity analysis

We investigated ROI-to-ROI correlations to assess similarity between ROI representations separately during encoding and recall. RSMs were constructed for each participant, using separate odd and even splits of the runs, based on Pearson correlations between voxel patterns for each pair of stimulus category. We conducted secondary correlations by correlating these correlation-based RSMs between each pair of ROIs (across odd and even splits), resulting in an ROI-to-ROI similarity matrix. This matrix was created by correlating the individual ROI RSMs calculated with half of the runs with the ones created using the other half of the runs, so we could also look to an ROI's similarity to itself across runs and

avoid any common fluctuations within runs (Henriksson et al., 2015). We additionally conducted multidimensional scaling (MDS), to visualize the similarity structure of these ROIs in two dimensions. This ROI-to-ROI similarity analysis was conducted separately for encoding trials and recall trials.

Whole-Brain Searchlights

We also conducted discriminability analyses using spherical searchlights (3-voxel radius) in two ways. First, we conducted discriminability analyses (as described above) for searchlights centered on voxels in the ROIs. For each searchlight, we obtained a scene-object discriminability metric during encoding and one during recall, allowing us to examine the relationship between encoding and recall information in these ROIs.

Second, we conducted discriminability analyses in searchlights iteratively moved through each individual's brain, to examine ability to discriminate information outside of our pre-defined ROIs. Group maps were combined with a two-tailed t-test comparing group discrimination indices versus no discrimination (0). Group maps were thresholded at $p < 0.01$ uncorrected for visualization purposes, however we also provide unthresholded maps. We conducted these searchlights looking at both discriminability of information within memory process type (encoding or recall), as well as ability to cross-discriminate (e.g., correlating encoding and recall patterns).

Modeling behavior

We conducted analyses to relate fMRI activity to behavioral measures of reported recall vividness and post-scan recognition performance. Additional GLMs were conducted with the fMRI data to obtain an estimate for each trial for each run, so that they could be compared with trial-by-trial behavior measures. We used support vector machines (SVMs) to measure the ability to classify later successful recognition versus failed recognition (hits vs. misses) from ROI patterns during encoding or recall. We also conducted SVMs to classify recall vividness responses (no memory, low vividness, high vividness) from ROI patterns during encoding or

recall. SVMs were conducted on all pairs of the three classes, and then classification accuracies were averaged. All SVMs were conducted using a leave-one-run-out approach.

Results

In the following sections, we present several analyses elucidating the relationship between representations elicited during encoding and recall. First, we investigate what stimulus-based content can be discriminated from encoding and recall response patterns in object- and scene-selective visual ROIs and the hippocampus. Second, we calculate the degree to which these patterns can be used to decode memory strength and performance for individual items. Third, we analyze the relationships between these ROIs to see how they change during encoding and recall. Finally, we conduct searchlight analyses to investigate the distribution of voxels showing the strongest discrimination during encoding, recall and between these two phases, both within and outside the ROIs.

Decoding stimulus content from scene- and object-selective visual regions and hippocampus

What aspects of a visual memory are represented in scene- and object-selective areas and hippocampus during encoding and recall? We asked this question by discriminating stimulus information from the patterns of blood oxygen level dependent (BOLD) responses at various scales of stimulus granularity, ranging from broad stimulus class (scenes, objects), to stimulus type (e.g., natural/manmade scene, big/small object), to specific stimulus category (e.g., cupcake, guitar). This discrimination was conducted across independent exemplars, never including the same images in the training and testing sets of the decoding model. This allowed us to see what levels of information are represented in these regions, separate from an ability to distinguish identical images.

Scene- and object-selective ROIs: Detailed information during encoding, limited information during recall

We investigated discriminability in object-selective regions LO and pFs and scene-selective regions PPA, MPA, and OPA (Figure 3). All regions could discriminate broad stimulus

class (objects vs. scenes) during encoding (LO: $t(21)=5.54$, $p=1.70 \times 10^{-5}$; pFs: $t(21)=5.41$, $p=2.28 \times 10^{-5}$; PPA: $t(21)=7.34$, $p=3.16 \times 10^{-7}$; MPA: $t(19)=6.36$, $p=4.18 \times 10^{-6}$; OPA: $t(20)=6.13$, $p=6.83 \times 10^{-6}$). Object type of tool/non-tool could be discriminated to an extent in object-selective regions LO ($t(21)=2.56$, $p=0.018$), and pFs ($t(21)=2.60$, $p=0.017$), although neither comparison passed FDR correction. Object size did not show significant discriminability in any region. Individual object categories could be discriminated in all regions (LO: $t(21)=3.02$, $p=0.006$; pFs: $t(21)=4.13$, $p=4.74 \times 10^{-4}$; PPA: $t(21)=3.00$, $p=0.007$; MPA: $t(19)=2.95$, $p=0.008$; OPA: $t(19)=3.99$, $p=7.78 \times 10^{-4}$). Scene types could also be decoded from most regions, including open/closed (LO: $t(21)=3.74$, $p=0.001$; pFs: $t(21)=4.14$, $p=4.61 \times 10^{-4}$; PPA: $t(21)=3.74$, $p=0.001$) and natural/manmade (LO: $t(21)=3.69$, $p=0.001$; pFs: $t(21)=3.60$, $p=0.002$; PPA: $t(21)=3.49$, $p=0.002$; MPA: $t(19)=4.06$, $p=6.65 \times 10^{-4}$). Finally, individual scene categories could also be discriminated in scene-selective regions PPA ($t(21)=2.86$, $p=0.009$) and OPA ($t(20)=3.52$, $p=0.002$). Overall, these results confirmed the findings of several prior studies (e.g., Valyear et al., 2007; Walther et al., 2009; Park et al., 2011; Kravitz et al., 2011; Troiani et al., 2012), in which responses in scene- and object-selective regions can be used to distinguish various levels of information about visually presented scenes and objects.

During recall, all high-level visual regions could distinguish recalled objects from scenes (LO: $t(21)=3.88$, $p=8.65 \times 10^{-4}$; pFs: $t(21)=3.17$, $p=0.005$; PPA: $t(21)=4.34$, $p=2.91 \times 10^{-4}$; MPA: $t(19)=2.82$, $p=0.011$; OPA: $t(20)=2.99$, $p=0.008$). No regions showed significant discriminability for object type (big/small, tool/non-tool) nor scene type (open/closed, natural/manmade) during recall. No region showed discrimination of object category, however the MPA showed significant discrimination of scene category during recall ($t(19)=3.23$, $p=0.004$). These results reveal that while multiple regions maintain information about broad stimulus class during recall and there is some information about individual category within the MPA, we found no evidence for decoding intermediate stimulus anywhere.

To investigate which regions show a shared neural representation during encoding and recall, we conducted a cross-discrimination analysis identifying the degree to which a region shows similar patterns between encoding and recall. The only significant cross-discrimination was for stimulus class (objects versus scenes) in the pFs ($t(21)=2.67$, $p=0.014$) and MPA

(*t*(19)=3.53, *p*=0.002). Significant cross-discrimination did not emerge for any finer-grained stimulus information in scene- and object-selective ROIs.

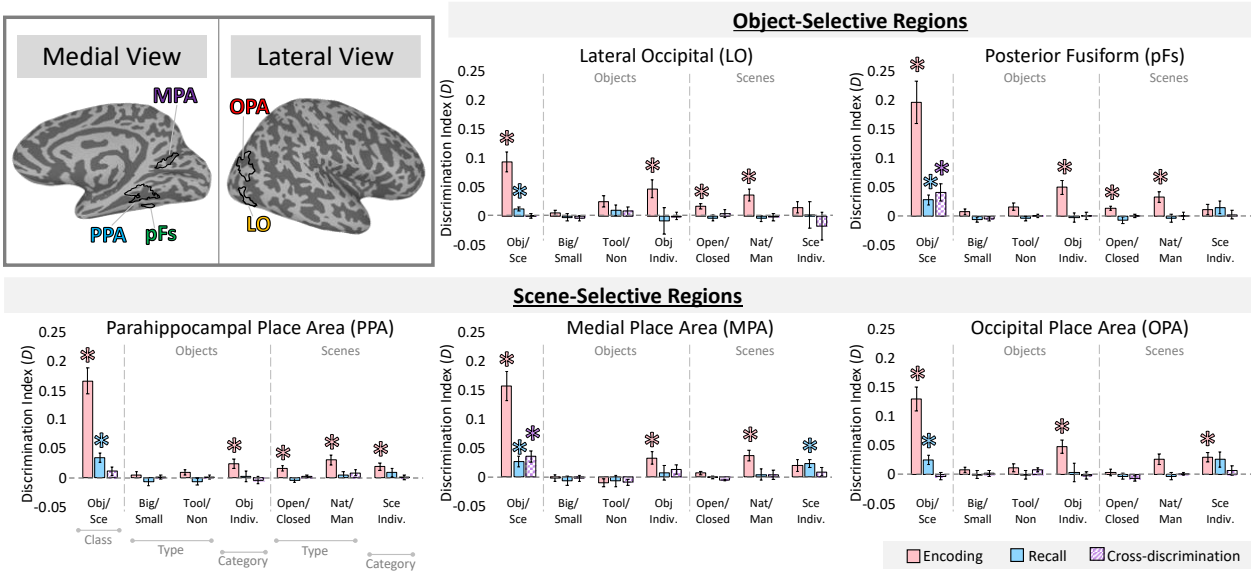

Figure 3 – **Information discriminability in scene- and object-selective regions.** Discriminability for scene- and object-selective regions of interest (ROIs) for each stimulus property was calculated from the RSMs (as in Figure 2). ROIs correspond to those shown in the upper left; shown here are probabilistic ROIs chosen as voxels shared by at least 12% participants, however analyses were conducted in individually localized ROIs. Bar graphs indicate mean discrimination index for different comparisons across ROIs, are split by broad stimulus class, and show three levels of discrimination: 1) broad discrimination of stimulus *class* (objects versus scenes), 2) mid-level discrimination of stimulus *type* (objects: big/small, tools/non-tools; scenes: open/closed, natural/manmade), and 3) fine-grained discrimination of stimulus *category* (object and scene individuation). The y-axis represents the average discrimination index (*D*), which ranges from -1 to 1 and can be compared to a null level of 0. Pink bars indicate discriminability during encoding trials, blue bars indicate discriminability during recall trials, and hatched purple bars indicate cross-discriminability (i.e., there is a shared representation between encoding and recall). Error bars indicate standard error of the mean. Asterisks (*) indicate significance at a FDR corrected level of $q<0.05$.

Hippocampus Shows Broad Stimulus Class Information During Encoding

We conducted the same analyses in hippocampal ROIs (Figure 4). During encoding, the Hip-HB showed significant discrimination of objects versus scenes ($t(21)=4.05$, $p=5.78 \times 10^{-4}$) However, the Hip-HB showed significant sensitivity to no other information during encoding. Interestingly, this pattern in the Hip-HB during encoding was similar to the scene- and object-

selective visual areas during recall, in their specific ability to discriminate broad stimulus class. The Hip-T showed no significant discriminability at any level during encoding. During recall, neither hippocampal region showed significant discriminability of any level of information (all $p>0.10$). No significant cross-discrimination between encoding and recall was observed (all $p>0.20$). Overall, the only information that emerged in the hippocampus was a difference between objects and scenes during encoding, and we found no evidence for discriminability of intermediate information, nor broad stimulus class (objects vs. scenes) during recall.

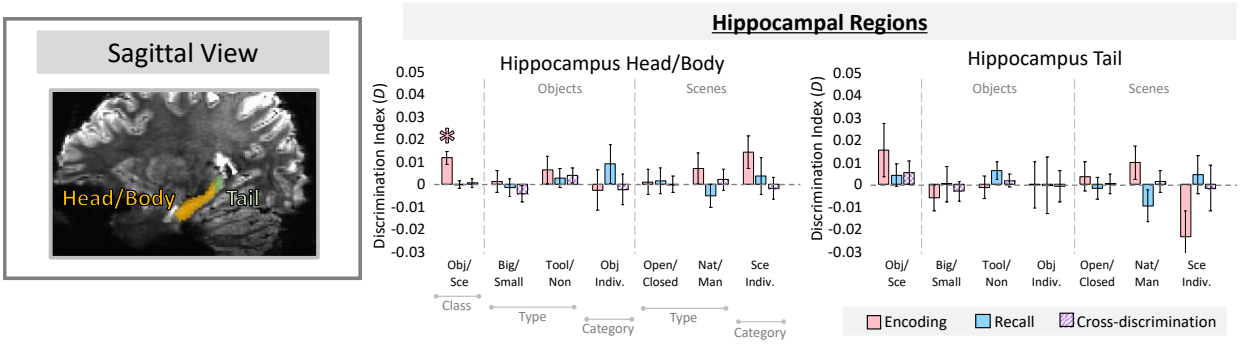

Figure 4 – **Information discriminability in the hippocampus**. Discriminability for hippocampal ROIs of each stimulus property was calculated from the RSMs. On the left is an example participant's 7T functional scan overlaid with their automatically segmented hippocampal regions (head/body and tail). Bar graphs are displayed in the same manner as Figure 3, and indicate mean discrimination index for comparisons of different levels of stimulus information (class, type, and category for objects and scenes). Pink bars indicate discriminability during encoding trials, blue bars indicate discriminability during recall trials, and hatched purple bars indicate cross-discriminability (i.e., there is a shared representation between encoding and recall). Error bars indicate standard error of the mean. Asterisks (*) indicate significance at a FDR corrected level of $q<0.05$.

Relationship of fMRI response patterns to memory behavior

In contrast to the specific visual content of a stimulus, to what degree do these regions represent information about the strength of the memory? We examined the ability to use the voxel values in each region to decode participant-reported memory vividness, a rating provided by participants after each recall trial in the scanner (Figure 5a). We also examined the ability to decode recognition success for each image based on a post-scan old/new recognition task (Figure 5b).

411

412 *FMRI response patterns and memory vividness*

413 Encoding patterns from all scene- and object-selective regions were predictive of recall
414 vividness: LO (M=62.28%, $t(21)=5.43$, $p=3.09 \times 10^{-5}$), pFs (M=60.90%, $t(21)=4.90$, $p=9.99 \times 10^{-5}$),
415 PPA (M=57.11%, $t(20)=4.99$, $p=8.12 \times 10^{-5}$), MPA (M=55.72%, $t(19)=2.40$, $p=0.027$), and OPA
416 (M=57.51, $t(20)=4.31$, $p=4.20 \times 10^{-4}$). In contrast, within the hippocampus, (Hip-HB and Hip-T),
417 encoding patterns could not be used to classify recall vividness (both $p>0.05$). Recall patterns
418 from all scene- and object-selective regions were also predictive of recall vividness: LO
419 (M=56.43%, $t(21)=4.22$, $p=4.61 \times 10^{-4}$), pFs (M=55.83%, $t(21)=3.36$, $p=0.003$), PPA (M=55.63%,
420 $t(19)=2.63$, $p=0.016$), MPA (M=57.50%, $t(19)=3.06$, $p=0.007$), and OPA (M=58.26%, $t(20)=3.85$,
421 $p=0.0012$). Additionally, the hippocampus showed memory vividness decodability from
422 patterns during recall, in both the Hip HB (M=53.34%, $t(21)=2.76$, $p=0.012$) and Hip T
423 (M=54.26%, $t(21)=2.49$, $p=0.022$). While hippocampus showed decodability during recall and
424 not during encoding, there was no significant difference in classification accuracy between
425 encoding and recall (both regions: $p>0.05$). These results indicate that scene- and object-
426 selective regions contain information about memory vividness during both encoding and recall,
427 while the hippocampus only contains information about memory vividness during the recall
428 period.

429

430 *FMRI response patterns and subsequent memory*

431 Encoding patterns from scene- and object-selective regions were predictive of later
432 successful recognition, from the LO (M=53.08%, $t(21)=2.31$, $p=0.032$), PPA (M=52.08%,
433 $t(21)=2.29$, $p=0.033$), and OPA (M=53.35%, $t(21)=3.86$, $p=0.001$). MPA, pFs, Hip HB and Hip T
434 did not show significant decodability of successful recognition (all $p>0.10$). No recall patterns
435 from any ROI were predictive of later successful recognition (all $p>0.10$). These results confirm
436 prior findings demonstrating an ability to predict subsequent memory performance from visual
437 areas (Brewer et al., 1998), and show little ability to decode later recognition success from
438 neural information during the recall period.

439

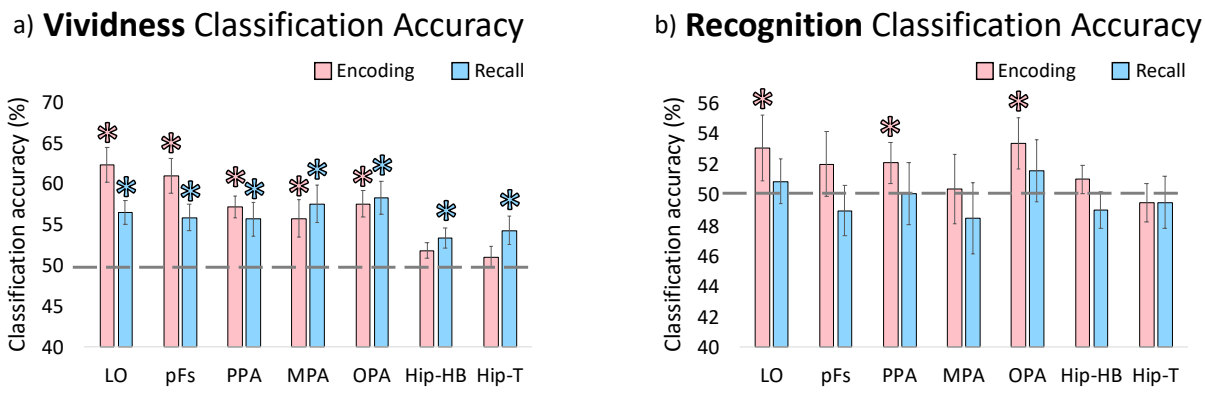

Figure 5 – **Relationship of fMRI response patterns to behavior.** (a) Classification accuracies for predicting subjectively reported recall vividness, based on patterns of encoding (pink) and recall (blue) from the ROIs. Chance level is 50%, and marked with the dashed grey line. Asterisks indicate a significantly higher classification accuracy than chance ($p < 0.05$). In scene- and object-selective visual regions, patterns during both encoding and recall can significantly predict the vividness of recall. In the hippocampus, only patterns during recall can significantly predict memory vividness. (b) Classification accuracies for predicting post-scan memory performance in a recognition task from patterns of encoding (pink) and recall (blue) from the ROIs. Only patterns from some scene- and object-selective regions during encoding (LO, PPA, OPA) show significant ability to predict later recognition success. No patterns during recall were linked with recognition success.

Region-to-region similarity during encoding and recall

Beyond investigating the stimulus content representations within individual regions, an equally important question is how these visual and memory regions relate to each other in their representations during encoding and recall. We looked at correlations of the RSMs between each pair of ROIs, separately for objects and scenes during both encoding and recall (Figure 6). These correlations were conducted using separate halves of the data, so diagonal values indicate an ROI's similarity to itself across runs of independent stimuli. We also conducted MDS to visualize the similarities across regions (Figure 6). For encoding objects and scenes, all regions were significantly self-correlated across runs (all p <0.001), indicating that these regions show consistent patterns across runs and exemplars. Within the MDS for encoding both objects and scenes, scene- and object-selective regions are grouped together, with object regions LO and pFs similar to each other, scene regions PPA and OPA similar to each other, and the MPA slightly dissimilar. Meanwhile, hippocampal regions are highly dissimilar from all scene- and object-selective regions.

During recall, the representational structure of these regions transforms. All ROIs are still significantly correlated with themselves for recalling objects and scenes (all $p < 0.001$). However, scene- and object-selective regions are more dissimilar from each other, and these regions and hippocampus are more similar (Figure 6). To quantify this cortical-hippocampal similarity, we compared the mean ranked correlation coefficient of the scene- and object-selective ROIs (pFs, LO, PPA, MPA, OPA) with the hippocampal ROIs (Hip-HB, Hip-T). In a 2-way ANOVA for stimulus category (object/scene) and memory process (encoding/recall), there was a significant difference of cortical-hippocampal similarity between encoding and recall ($F(1,84)=11.24$, $p=0.003$), but no main effect of stimulus category ($F(1,84)=3.13$, $p=0.09$) nor an interaction ($F(1,84)=0.78$, $p=0.388$). A post-hoc t-test indicated that cortical-hippocampal similarity was significantly higher during recall than encoding ($t(43) = 3.92$, $p=3.13 \times 10^{-4}$). Thus, across both objects and scenes, representations in scene- and object-selective cortex and hippocampus are more similar during recall than encoding.

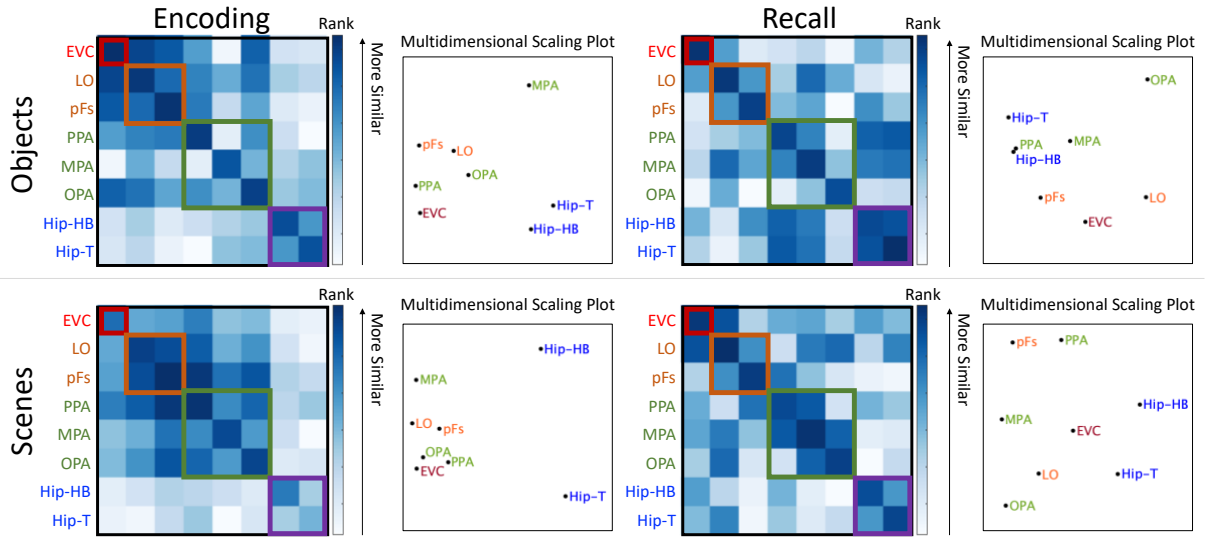

Figure 6 – **Comparison of stimulus representations between regions.** Matrices indicating Pearson correlations between the RSMs of every ROI pair, using separate halves of the data. Matrices for encoding and recall are shown separately for objects and scenes. In the matrices, dark blue indicates the most similar ROIs, while white indicates the most dissimilar ROIs. ROIs can be conceptually divided into four groups as indicated by the colored squares – early visual areas (red: EVC), object-selective areas (orange: LO, pFs), scene-selective areas (green: PPA, MPA, OPA), and hippocampus (blue: Hip-HB, Hip-T). Next to the encoding and recall RSMs are multidimensional scaling

(MDS) plots, which transform a given RSM into a two-dimensional representation where shorter distances indicate higher similarity. With this, one can visualize which ROIs have similar representations to another. During encoding, while hippocampal regions (blue) are very distinct in their representations from visual regions, they become more similar to visual regions during recall.

Direct comparison of encoding and recall discriminability in scene- and object-selective ROIs and hippocampus

If we directly compare the ability to discriminate information during encoding and recall, do we find a correlation or an overlap in discriminability? We conducted a discriminability analysis in 3-voxel radius spherical searchlights throughout the scene- and object-selective and hippocampal ROIs to see whether there were differences in which searchlights could best discriminate encoding information versus recall information. Given that these regions only showed discriminability for broad stimulus class (scenes, objects) during recall, we focused on this specific comparison in our searchlight. LO and MPA showed weak but significant correlations between encoding and recall discriminability (LO: Mean Spearman's rank correlation, ρ=0.08, Wilcoxon rank sum test: Z=2.22, p=0.026; MPA: ρ=0.15, Z=2.13, p=0.033). However, no other region showed a significant correlation, including PPA (ρ=0.08, Z=1.70, p=0.088), OPA (ρ=0.10, Z=1.46, p=0.145), pFs (ρ=0.13, Z=1.74, p=0.082), Hip-HB (ρ=0.05, Z=1.51, p=0.131), and Hip-T (ρ=0.06, Z=0.89, p=0.372). These results suggest that the strength of discriminability during recall is not predicted by the strength of discriminability during encoding.

To investigate this further, we focused on the top 10% of searchlights that showed encoding discriminability and compared them with the top 10% of searchlights that showed recall discriminability within each ROI (Figure 7). PPA, MPA, OPA, Hip-HB and Hip-T all revealed limited overlap of these encoding-recall searchlights that was not significantly different from a chance level of 10% (PPA: M=9.29%, SD=8.86%; MPA: M=19.45%, SD=19.79%; OPA: M=7.49%, SD=10.86%; Hip-HB: M=14.75%, SD=12.31%; Hip-T: M=17.38%, SD=14.02%). LO and pFs showed a significantly higher level of overlap than predicted by chance (LO: M=13.59%, SD=9.21%, Wilcoxon rank sum test: Z=2.08, p=0.038; pFS: 22.61%, SD=19.13%, Z=2.05, p=0.040); however, note that these results still show a relatively small overlap, with the majority of the top voxel-

centered searchlights (over 77%) showing specificity to either encoding or recall discriminability and not both.

These results suggest some degree of segregation between voxels that maintain encoding information and those that maintain recall information.

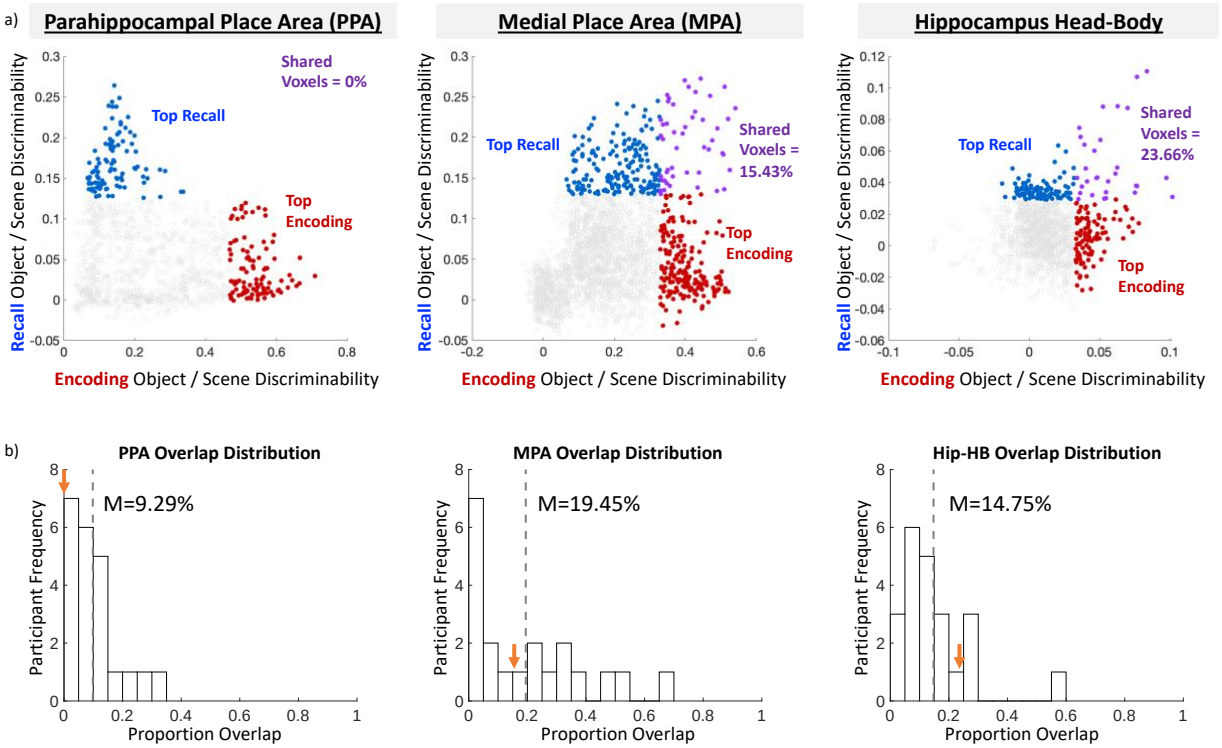

Figure 7 – **Comparing encoding and recall discriminability within the ROIs.** (a) Example ROIs from a single example participant, where each point represents a voxel-centered spherical searchlight in that ROI and is plotted by the object/scene discrimination index during encoding (x-axis) versus the object/scene discrimination index during recall (y-axis). The top 10% of searchlights showing recall discriminability are colored in blue, while the top 10% of searchlights showing encoding discriminability are colored in red. Searchlights that overlap between the two (those that demonstrate both encoding and recall discrimination) are colored in purple. Note that while the PPA shows no overlap for this participant, MPA and Hip-HB show greater overlap. However, all mean overlaps across regions remain below 22.61%. (b) Histograms for these ROIs showing participant distribution of the proportion of overlap between the top 10% of encoding discriminating and top 10% of recall discriminating voxels. The orange arrow represents the participant's data plotted in (a), while the dashed grey line shows the mean overlap, with proportion reported. Note that in general, there is low overlap across participants and regions in the top voxels for encoding and those for recall.

Whole-Brain Investigation of Encoding and Recall Effects

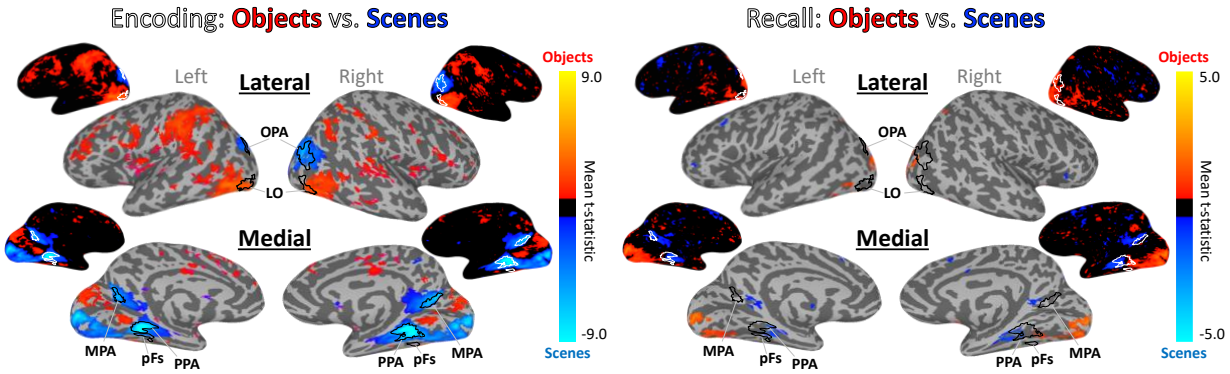

Figure 8 – **Whole-brain activation of objects and scenes during encoding and recall.** Univariate whole-brain t-statistic maps of the contrast of objects (red/yellow) versus scenes (blue/cyan) in encoding (left) and recall (right). Contrasts show group surface-aligned data (N=22), presented on the SUMA 141-subject standard surface brain (Saad and Reynolds, 2012). Outlined ROIs are defined by voxels shared by at least 25% participants from their individual ROI definitions (using independent functional localizers), with the exception of the pFs and OPA which were defined by 13% overlap (there were no voxels shared by 25% of participants). The encoding maps are thresholded at FDR corrected $q<0.05$. For the recall maps, no voxels passed FDR correction, so the contrast presented is thresholded at $p<0.01$ for visualization purposes. Smaller surface maps show unthresholded results.

Given the differences we observed between encoding and recall within ROIs, we conducted follow-up analyses at the whole-brain level. Looking at a group univariate contrast of objects versus scenes during encoding (Figure 8), we confirm that stimulus class selectivity is strongest in ROIs predicted by the literature: LO and pFs show high sensitivity to objects, while PPA, MPA, and OPA show high sensitivity to scenes (e.g., Epstein and Kanwisher, 1998; Grill-Spector et al., 2001). However, a group univariate contrast of objects versus scenes during recall reveals that recall scene-selectivity is strongest in areas anterior to PPA and MPA, and recall object-selectivity is strongest in areas anterior to LO and in early visual cortex. Rather than the peaks of recalled category overlapping with those of encoding, the greatest scene-object differences occur in a spatially separate set of voxels largely anterior to those during encoding.

A searchlight analysis looking at information discriminability across the brain replicates this spatial separation (Figure 9). During encoding, scenes and objects are most discriminable in

the same regions identified by the independent perceptual localizer (LO, pFS, PPA, MPA, OPA). However, during recall, peak discriminability occurs in voxels anterior to these regions, especially for the PPA, MPA, and left LO and OPA. Next, we employed a cross-discrimination searchlight to identify regions with shared stimulus representations between encoding and recall. Again, areas anterior to those most sensitive during encoding showed highest similarity between encoding and recall representations.

These results suggest a spatial separation between encoding and recall with strongest reinstatement occurring outside of scene- and object-selective regions typically localized in visual tasks.

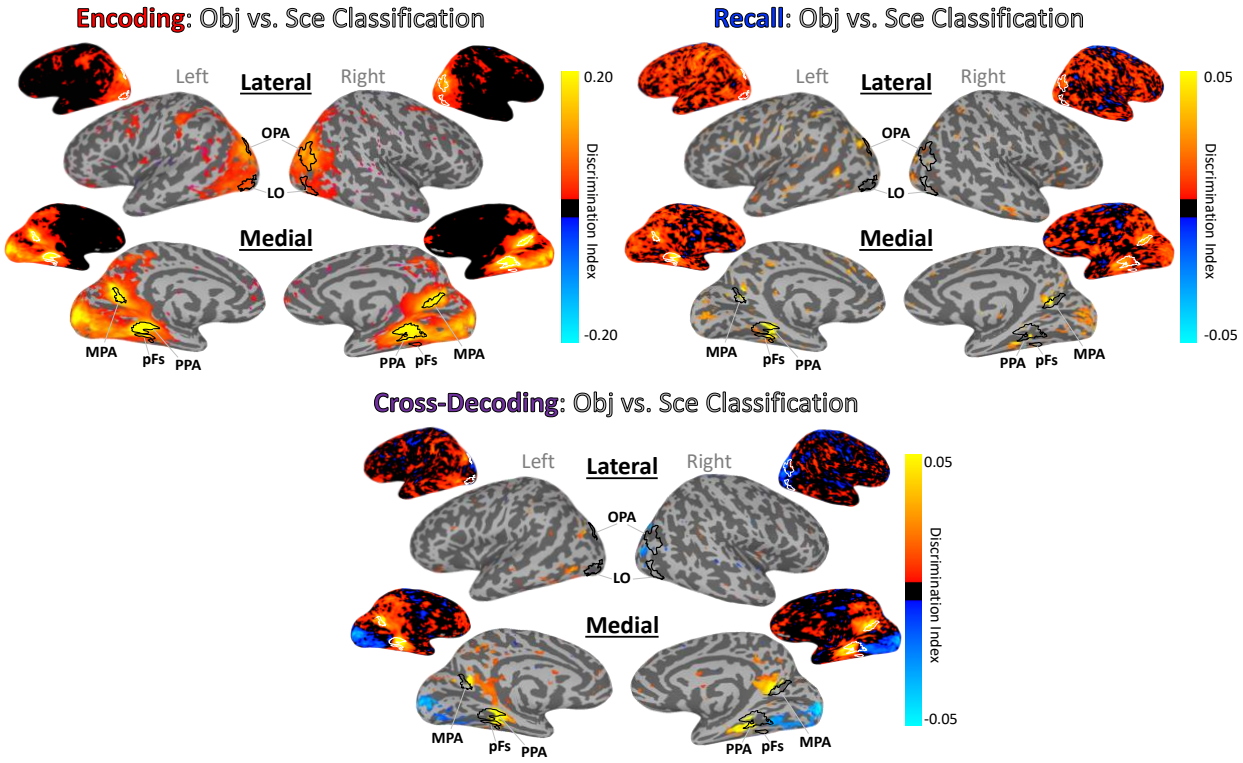

Figure 9 – **Whole-brain discrimination analyses for encoding, recall, and cross-decoding of information.** Whole-brain searchlight analyses investigating discrimination of objects versus scenes during encoding (top left), recall (top right), and cross-discrimination (bottom). Brighter yellows indicate higher discrimination indices. Outlined ROIs are defined using independent stimuli in an independent localizer run. All maps are thresholded at $p<0.01$ uncorrected, and unthresholded maps are also shown. The cross-discrimination searchlight shows regions that have a shared representation between encoding and recall.

Discussion

In this work, we conducted an in-depth investigation of how and where recalled memory content for complex object and scene images is represented in the brain. First, we observed a striking difference in the granularity of representations in cortex between encoding and recall. While information in cortex during encoding reflected multiple levels of information, during recall we observed coarse level information (objects versus scenes) only. Second, a direct comparison between encoding and recall discriminability within cortical and hippocampal ROIs found no correlation. Further, there was a segregation between the subregions containing the most information during encoding and those during recall. Third, there was an increase in the similarity between hippocampal and cortical regions from encoding to recall. Finally, a whole brain comparison of encoding and recall discriminability revealed that the peaks for recall as well as the strongest encoding-recall similarity were spatially anterior to the peaks during encoding. Collectively, our results reveal key spatial and representational differences between encoding and recalling stimulus content.

The ability to decode scenes versus objects during recall is consistent with several findings showing broad stimulus class decodability during recall (Polyn et al., 2005; Reddy et al., 2010; Boccia et al., 2019; O'Craven and Kanwisher, 2000). Additionally, we replicate several findings observing discriminability of different levels of information during perception (e.g., Mahon et al., 2007; Walther et al., 2009 Kravitz et al., 2011; Park et al., 2011; Konkle et al., 2012). We also find a significant ability to decode memory vividness and future recognition success from many cortical regions as shown in prior work (Brewer et al., 1998; Wais, 2008; Dijkstra et al., 2017; Fulford et al., 2018). However, at face-value our findings appear to be at odds with prior work that reported fine-grained information during recall as well as encoding-recall similarity in category-selective cortex. We discuss each of these issues in turn in the paragraphs below.

In terms of fine-grained information during recall, prior work has reported an ability to decode individual items (Chadwick et al., 2010; Lee et al., 2012; Kuhl and Chun, 2014; Wing et al., 2015; Mack and Preston, 2016; Tompary et al., 2016). However, in these studies, the

information decoded could reflect image-specific features and not necessarily a general representation of the items. In our study, we specifically tested for generalizable stimulus content representations and not individual images, never comparing encoding or recalling an image with itself. Instead, we compared representations across exemplars to minimize the contribution of image-specific features. The resulting inability to detect fine-grained information during recall suggests that imagery-based representations in scene- and object-selective visual areas may not contain more abstracted or generalized levels of information. Instead, participants may be recalling limited image features, sufficient for image-level classification or classification at the broad level of scenes versus objects (given large differences between their features), but not more abstracted classifications like base-level category (e.g., living room), or properties (e.g., natural or manmade).

In terms of encoding-recall similarity, our results also appear to be inconsistent with some previous findings of sensory reinstatement, in which the neurons or voxels sensitive during encoding have been reported to show the same patterns during recall (Danker and Anderson, 2010; Buchsbaum et al., 2012; Johnson and Johnson, 2014; Schultz et al., 2019). Within scene- and object-selective cortex, we observed limited overlap between the sub-regions with peak encoding and those with peak recall information, with the strongest encoding-recall similarity in more anterior regions. These results are not in conflict with many studies reporting encoding-recall similarity in areas outside of category-selective cortex such as the medial temporal lobe (e.g., Tompary et al., 2016; Schultz et al., 2019). However, some studies do report encoding-recall similarity within scene- and object-selective cortex (e.g., O'Craven and Kanwisher, 2000; Johnson and Johnson, 2014) which may be attributable to key methodological differences from the current study. First, as noted above, we targeted recollection of stimulus content rather than individual items. While scene- and object-selective regions may maintain item-specific visual information during both encoding and recall, our results suggest a difference in representations during encoding and recall at more generalized levels of information. Second, we employed an item-based recall task, rather than associative tasks commonly used to study recall (e.g., Ganis et al., 2004; Zeidman et al., 2015a; Jonker et

al., 2018). This allowed us to ensure that information we decoded was not related to other factors such as decoding a cue or association.

Our findings suggest a posterior-anterior gradient within cortical regions, in which recalled representations extend anterior to encoding or perceptual representations. These results agree with recent research showing that regions involved in scene memory are anterior to those involved in scene perception, with the possibility of separate perception and memory networks (Baldassano et al., 2016; Burles et al., 2018; Chrastil, 2018; Silson et al., 2019a). This anterior bias for recall may reflect top-down refreshing of a memory representation in contrast to the largely bottom-up processes that occur during perception (Mechelli et al., 2004; Johnson et al., 2007; Dijkstra et al., 2019). Alternatively, other work has suggested a gradient within the neocortex that reflects a split of conceptual information represented anterior (or downstream) to perceptual information (Peelen and Caramazza, 2012; Borghesani et al., 2016; Martin, 2016). While recent work shows highly detailed visual content within recalled memories (Bainbridge et al., 2019), it is possible recalled memories may be more abstracted and conceptual compared to their encoded representations. This recalled memory could thus contain less fine-grained perceptual information or be abstracted into a different representation, explaining why we can decode memory strength but not fine-grained perceptually-defined distinctions (e.g., natural versus manmade) during recall. Collectively, our results support these two possible accounts for anterior-posterior gradients of memory/perception or conceptual/perceptual information in the brain, in contrast with other accounts claiming an identical representation between encoding and recall (e.g., Schultz et al., 2019).

The current work also provides further support for a content-independent role of the hippocampus in memory. During encoding, we observe broad content selectivity in the hippocampus, as has been observed in other recent work claiming a perceptual role for the hippocampus (Zeidman et al., 2015b; Hodgetts et al., 2017). However, we do not observe strong evidence of any other content representations during encoding or recall; the hippocampus does not show sensitivity to more fine-grained information, and during recall, it does not even show differences at the broadest distinction of objects versus scenes. These results lend support for the notion that the hippocampus is largely content-independent

(Davachi, 2006; Danker and Anderson, 2010; Liang et al., 2013; Schultz et al., 2019), with individual item decoding in previous work possibly driven by decoding of indexes within the hippocampus connected to fuller representations in the neocortex, or a coding of memory strength (e.g., Teyler and Rudy, Jonker et al., 2018). In fact, while stimulus content during recall is not discriminable, we find that memory strength is decodable from the hippocampus, mirroring similar results finding strength but not content representations in the hippocampus for oriented gratings (Bosch et al., 2014). There is also evidence to suggest that the hippocampus may require longer delays (e.g., several hours to a day) to develop decodable representations of memory content (Lee et al., 2019) and this issue will require examination in future work.

The current study combining nested categorical structure for real-world images and an item-based recall approach allows us to observe different levels of stimulus representations across the brain; however, there are limitations to this methodology that could be addressed in future work. First, the relative lack of fine-grained information during recall could partly reflect a lack of power that could benefit from a larger stimulus set or a memory task that emphasizes these different stimulus properties. However, it is important to note that we are able to decode memory strength from these regions, as well as both broad stimulus class and fine-grained stimulus category (but not intermediate information) from the MPA, suggesting that the difference between encoding and recall is not simply a question of power. In fact, the current sample size (N=22) falls in the higher range compared to related studies (e.g., Lee et al., 2012: N=11; Johnson and Johnson, 2014: N=16; Schultz et al., 2019: N=16). Second, while our current methodology allows us to powerfully test stimulus content divorced from memory for individual items, this means we cannot assess discriminability for individual images. Future studies should investigate whether individual item representations are identical between encoding and recall, even if more general content representations are not. Such findings could have meaningful implications on the nature of representations during recall, suggesting the imagery for an individual item is vivid enough to be item-specific, but results in a limited level of abstraction. Finally, it will be important to see whether these newly defined anterior recall regions show more fine-grained representations of stimulus content during recall, and whether

693 there may be region-specific differences (e.g., the MPA in particular has been a key target for
694 comparisons of scene perception and scene recall; Burles et al., 2018; Chrastil, 2018; Silson et
695 al., 2019b).
696 Examining item-based recall and representations of memory content in the brain has
697 ultimately unveiled a rather complex, nuanced relationship of encoding and recall, with
698 strongest encoding-recall similarity occurring largely anterior to scene- and object-selective
699 visual cortex. In the study of memory, it is important to examine now only how we remember,
700 but *what* we are remembering, and this study reveals that the way in which this content is
701 manifested may vary greatly between encoding and recall.
702
703 References
704
705 Bainbridge WA, Oliva A (2015) Interaction envelope: Local spatial representations of objects at
706 all scales in scene-selective regions. Neuroimage 122:408-416.
707
708 Bainbridge WA, Hall EH, Baker CI (2019) Drawings of real-world scenes during free recall reveal
709 detailed object and spatial information in memory. Nat Commun 10:5.
710
711 Baldassano C, Esteva A, Fei-Fei L, Beck DM (2016) Two distinct scene-processing networks
712 connecting vision and memory. eNeuro 3:ENEURO.0178-16.2016.
713
714 Beauchamp MS, Martin A (2007) Grounding object concepts in perception and action: Evidence
715 from fMRI studies of tools. Cortex 43:461-468.
716
717 Boccia M, Sulpizio V, Teghil A, Palermo L, Piccardi L, Galati G, Guariglia C (2019) The dynamic
718 contribution of the high-level visual cortex to imagery and perception. Hum Brain Mapp
719 40:2449-2463.
720

721 Borghesani V, Pedregosa F, Buiatti M, Amaxon A, Eger E, Piazza M (2016) Word meaning in the
722 ventral visual path: a perceptual to conceptual gradient of semantic coding. Neuroimage
723 143:128-140.
724
725 Bosch SE, Jehee JFM, Fernández G, Doeller CF (2014) Reinstatement of associative memories in
726 early visual cortex is signaled by the hippocampus. J Neurosci 34:7493-7500.
727
728 Brewer JB, Zhao Z, Desmond JE, Glover GH, Gabrieli JDE (1998) Making memories: Brain activity
729 that predicts how well visual experience will be remembered. Science 281:1185-1187.
730
731 Brodt S, Gais S, Beck J, Erb M, Scheffler K, Shönauer M (2018) Fast track to the neocortex: A
732 memory engram in the posterior parietal cortex. Science 362:1045-1048.
733
734 Buckner RL, Wheeler ME (2001) The cognitive neuroscience of remembering. Nat Rev Neurosci
735 2:624.
736
737 Burles F, Ultimá A, McFarlane LH, Potocki K, Iara G (2018) Ventral-dorsal functional contribution
738 of the posterior cingulate cortex in human spatial orientation: A meta-analysis. Front Hum
739 Neurosci 12:190.
740
741 Buschbaum BR, Lemire-Rodger S, Fang C, Abdi H (2012) The neural basis of vivid memory is
742 patterned on perception. J Cogn Neurosci 24:1867-1883.
743
744 Chadwick MJ, Hassabis D, Weiskopf N, Maguire E (2010) Decoding individual episodic memory
745 traces in the human hippocampus. Curr Biol 20:544-547.
746
747 Chrastil ER (2018) Hetereogeneity in human retrosplenial cortex: A review of function and
748 connectivity. Behav Neurosci 132:317-338.
749

Cichy RM, Pantazis D, Oliva A (2014) Resolving human object recognition in space and time. Nat Neurosci 17:455.

Cox RW (1996) AFNI: Software for analysis and visualization of functional magnetic resonance neuroimages. Comput Biomed Res 29:162-173.

Danker JF, Anderson JR (2010) The ghosts of brain states past: Remembering reactivates the brain regions engaged during encoding. Psychol Bull 136:87.

Davachi L, Mitchell JP, Wagner AD (2003) Multiple routes to memory: Distinct medial temporal lobe processes build item and source memories. Proc Natl Acad Sci USA 100:2157-2162.

Davachi L (2006) Item, context and relational episodic encoding in humans. Curr Opin Neurobiol 16:693-700.

Dickerson BC, Miller SL, Greve DN, Dale AM, Albert MS, Schacter DL, Sperling RA (2007) Prefrontal-hippocampal-fusiform activity during encoding predicts intraindividual differences in free recall ability: an event-related functional-anatomic MRI study. Hippocampus 17:1060-1070.

Dijkstra N, Bosch SE, van Gerven MA (2017) Vividness of visual imagery depends on the neural overlap with perception in visual areas. J Neurosci 37:1367-1373.

Dijkstra N, Bosch SE, van Gerven MAJ (2019) Shared neural mechanisms of visual perception and imagery. Trends Cogn Sci 23:423-434.

Dilks DD, Julian JB, Paunov AM, Kanwisher N (2013) The occipital place area is causally and selectively involved in scene perception. J Neurosci 33:1331-1336.

778 Epstein R, Kanwisher N (1998) A cortical representation of the local visual environment. Nature
779 392:598.
780
781 Fulford J, Milton F, Salas D, Smith A, Simler A, Winlove C, Zeman A (2018) The neural correlates
782 of visual imagery vividness – an fMRI study and literature review. Cortex 105:26-40.
783
784 Ganis G, Thompson WL, Kosslyn SM (2004) Brain areas underlying visual mental imagery and
785 visual perception: an fMRI study. Cogn Brain Res 20:226-241.
786
787 Gelbard-Sagiv H, Mukamel R, Harel M, Malach R, Fried I (2008) Internally generated reactivation
788 of single neurons in human hippocampus during free recall. Science 322:96-101.
789
790 Gold JJ, Hopkins RO, Squire LR (2006) Single-item memory, associative memory, and the human
791 hippocampus. Learn Mem 13:644-649.
792
793 Grèzes J, Tucker M, Armony J, Ellis R, Passingham RE (2003) Objects automatically potentiate
794 action: an fMRI study of implicit processing. Eur J Neurosci 17:2735-2740.
795
796 Grill-Spector K, Kourtzi Z, Kanwisher N (2001) The lateral occipital complex and its role in object
797 recognition. Vis Res 41:1409-1422.
798
799 Harel A, Kravitz DJ, Baker CI (2013) Deconstructing visual scenes in cortex: Gradients of object
800 and spatial layout information. Cereb Cortex 23:947-957.
801
802 Harel A, Kravitz DJ, Baker CI (2014) Task context impacts visual object processing differentially
803 across the cortex. Proc Natl Acad Sci USA. 111:E962-E971.
804
805 Henriksson L, Khaligh-Razavi S-M, Kay K, Kriegeskorte N (2015) Visual representations are
806 dominated by intrinsic fluctuations correlated between areas. NeuroImage 114:275-286.

Hodgetts CJ, Voets NL, Thomas AG, Clare S, Lawrence AD, Graham KS (2017) Ultra-high-field fMRI reveals a role for the subiculum in scene perceptual discrimination. J Neurosci 37:3150-3159.

Huffman DJ, Stark CE (2014) Multivariate pattern analysis of the human medial temporal lobe revealed representationally categorical cortex and representationally agnostic hippocampus. Hippocampus 24:1394-1403.

Iglesias JE, Augustinack JC, Nguyen K, Player CM, Player A, Wright M, Roy N, Frosch MP, McKee AC, Wald LL, Fischl B, van Leemput K (2016) A computational atlas of the hippocampal formation using ex vivo, ultra-high resolution MRI: Application to adaptive segmentation of in vivo MRI. Neuroimage 115:117-137.

Ishai A, Ungerleider LG, Haxby JV (2000) Distributed neural systems for the generation of visual images. Neuron 28:979-990.

Ison MJ, Quiroga RQ, Fried I (2015) Rapid encoding of new memories by individual neurons in the human brain. Neuron 87:220-230.

Johnson MR, Mitchell KJ, Raye CL, D'Esposito M, Johnson MK (2007) A brief thought can modulate activity in extrastriate visual areas: Top-down effects of refreshing just-seen visual stimuli. Neuroimage 37:290-299.

Johnson JD, McDuff SG, Rugg MD, Norman KA (2009) Recollection, familiarity, and cortical reinstatement: A multivoxel pattern analysis. Neuron 63:697-708.

Johnson MR, Johnson MK (2014) Decoding individual natural scene representations during perception and imagery. Front Hum Neurosci 8:59.

Jonker TR, Dimsdale-Zucker H, Ritchey M, Clarke A, Ranganath C (2018) Neural reactivation in parietal cortex enhances memory for episodically linked information. Proc Natl Acad Sci USA 115:11084-11089.

Kahn I, Davachi L, Wagner AD (2004) Functional-neuroanatomic correlates of recollection: Implications for models of recognition memory. J Neurosci 24:4172-4180.

Konkle T, Oliva A (2012) A real-world size organization of object responses in occipitotemporal cortex. Neuron 74:1114-1124.

Kravitz DJ, Peng CS, Baker CI (2011) Real-world scene representations in high-level visual cortex: It's the spaces more than the places. J Neurosci 31:7322-7333.

Kriegeskorte N, Mur M, Bandettini P (2008) Representational similarity analysis – connecting the branches of systems neuroscience. Front Syst Neurosci 2:4.

Kuhl BA, Rissman J, Wagner AD (2012) Multi-voxel patterns of visual category representation during episodic encoding are predictive of subsequent memory. Neuropsychologia 50:458-469.

Kuhl BA, Chun MM (2014) Successful remembering elicits event-specific activity patterns in lateral parietal cortex. J Neurosci 34:8051-8060.

LaRocque KF, Smith ME, Carr VA, Witthoft N, Grill-Spector K, Wagner AD (2013) Global similarity and pattern separation in the human medial temporal lobe predict subsequent memory. J Neurosci 33:5466-5474.

Lee SH, Kravitz DJ, Baker CI (2012) Disentangling visual imagery and perception of real-world objects. Neuroimage 59:4064-4073.

Lee SH, Kravitz DJ, Baker CI (2019) Differential representations of perceived and retrieved visual information in hippocampus and cortex. Cereb Cortex 29:4452-4461.

Lewis JW (2006) Cortical networks related to human use of tools. Neuroscientist 12:211-231.

Liang JC, Wagner AD, Preston AR (2013) Content representation in the human medial temporal lobe. Cereb Cortex 23:80-96.

Mack ML, Preston AR (2016) Decisions about the past are guided by reinstatement of specific memories in the hippocampus and perirhinal cortex. Neuroimage 127:144-157.

Mahon BZ, Milleville SSC, Negri GAL, Rumiati RI, Caramazza A, Martin A (2007) Action-related properties shape object representations in the ventral stream. Neuron 55:507-520.

Martin A (2016) GRAPES—Grounding representations in action, perception, and emotion systems: How object properties and categories are represented in the human brain. Psychon Bull Rev 23:979-990.

McClelland JL, McNaughton BL, O'Reilly RC (1995) Why there are complementary learning systems in the hippocampus and neocortex: Insights from the successes and failures of connectionist models of learning and memory. Psychol Rev 102:419.

Mechelli A, Price CJ, Friston KJ, Ishai A (2004) Where bottom-up meets top-down: Neuronal interactions during perception and imagery. Cereb Cortex 14:1256-1265.

O'Craven KM, Kanwisher N (2000) Mental imagery of faces and places activates corresponding stimulus-specific brain regions. J Cogn Neurosci 12:1013-1023.

894 Park S, Brady TF, Greene MR, Oliva A (2011) Disentangling scene content from spatial boundary:
895 Complementary roles for the parahippocampal place area and lateral occipital complex in
896 representing real-world scenes. J Neurosci 31:1333-1340.
897
898 Peelen MV, Caramazza A (2012) Conceptual object representations in human anterior temporal
899 cortex. J Neurosci 32:15728-15736.
900
901 Polyn SM, Natu VS, Cohen JD, Norman KA (2005) Category-specific cortical activity precedes
902 retrieval during memory search. Science 310:1963-1966.
903
904 Ranganath C, Ritchey M (2012) Two cortical systems for memory-guided behavior. Nat Rev
905 Neurosci 13:713-726.
906
907 Reddy L, Tsuchiya N, Serre T (2010) Reading the mind's eye: Decoding category information
908 during mental imagery. Neuroimage 50:818-825.
909
910 Ritchey M, Wing EA, LaBar KS, Cabeza R (2012) Neural similarity between encoding and
911 retrieval is related to memory via hippocampal interactions. Cereb Cortex 23:2818-2828.
912
913 Ross DA, Sadil P, Wilson DM, Cowell RA (2017) Hippocampal engagement during recall depends
914 on memory content. Cereb Cortex 28:2685-2698.
915
916 Rugg MD, King DR (2018) Ventral lateral parietal cortex and episodic memory retrieval. Cortex
917 107:238-250.
918
919 Saad ZS, Reynolds RC (2012) SUMA. Neuroimage 62:768-773.
920
921 Schultz H, Tibon R, LaRocque KF, Gagnon SA, Wagner AD, Staresina BP (2019) Content tuning in
922 the medial temporal lobe cortex: Voxels that perceive, retrieve. eNeuro. 6.

Silson EH, Steel AD, Baker, CI (2016) Scene-selectivity and retinotopy in medial parietal cortex. Front Hum Neurosci 10:412.

Silson EH, Steel A, Kidder A, Gilmore AW, Baker CI (2019a) Distinct subdivisions of human medial parietal cortex support recollection of people and places. eLife 8.

Silson EH, Gilmore AW, Kalinowski SE, Steel A, Kidder A, Martin A, Baker, CI (2019b) A posterior-anterior distinction between scene perception and scene construction in human medial parietal cortex. J Neurosci 39:705-717.

Staresina BP, Davachi L (2006) Differential encoding mechanisms for subsequent associative recognition and free recall. J Neurosci 26:9162-9172.

Staresina BP, Henson RN, Kriegeskorte N, Alink A (2012) Episodic reinstatement in the medial temporal lobe. J Neurosci 32:18150-18156.

Sullivan Giovanello K, Schnyer DM, Verfaellie M (2003) A critical role for the anterior hippocampus in relational memory: Evidence from an fMRI study comparing associative and item recognition. Hippocampus 14:5-8.

Teyler TJ, Rudy JW (2007) The hippocampal indexing theory and episodic memory: Updating the index. Hippocampus 17:1158-1169.

Tompary A, Duncan K, Davachi L (2016) High-resolution investigation of memory-specific reinstatement in the hippocampus and perirhinal cortex. Hippocampus 26:995-1007.

Troiani V, Stigliani A, Smith ME, Epstein RA (2012) Multiple object properties drive scene-selective regions. Cereb Cortex 24:883-897.

952

953 Valyear KF, Cavina-Pratesi C, Stiglick AJ, Culham J (2007) Does tool-related fMRI activity within
954 the intraparietal sulcus reflect the plan to grasp? Neuroimage 36:T94-T108.
955
956 Vilberg KL, Rugg MD (2009) Functional significance of retrieval-related activity in lateral parietal
957 cortex: Evidence from fMRI and ERPs. Hum Brain Map 30:1490-1501.
958
959 Wais PE (2008) fMRI signals associated with memory strength in the medial temporal lobes: A
960 meta-analysis. Neuropsychologia 46:3185-3196.
961
962 Walther DB, Caddigan E, Fei-Fei L, Beck DM (2009) Natural scene categories revealed in
963 distributed patterns of activity in the human brain. J Neurosci 29:10573-10581.
964
965 Wing EA, Ritchey M, Cabeza R (2015) Reinstatement of individual past events revealed by the
966 similarity of distributed activation patterns during encoding and retrieval. J Cogn Neurosci
967 27:679-691.
968
969 Xiao X, Dong Q, Gao J, Men W, Poldrack R, Xue G (2017) Transformed neural pattern
970 reinstatement during episodic memory retrieval. J Neurosci 37:2986-2998.
971
972 Zeidman P, Lutti A, Maguire EA (2015a) Investigating the functions of subregions within anterior
973 hippocampus. Cortex 73:240-256.
974
975 Zeidman P, Mullally SL, Maguire EA (2015b) Constructing, perceiving, and maintaining scenes:
976 hippocampal activity and connectivity. Cereb Cortex 252:3836-3855.
977
978 Zeineh MM, Engel SA, Thompson PM, Bookheimer SY (2003) Dynamics of the hippocampus
979 during encoding and retrieval of face-name pairs. Science 299:577-580.
980